JOURNAL OF COMPUTATIONAL PHYSICS 57, 129–136 (1985)

Flux-Corrected Transport and Diffusion on a Non-Uniform Mesh

R. MORROW AND L. E. CRAM

CSIRO Division of Applied Physics, Sydney, Australia 2070

Received August 24, 1982; revised March 21, 1984

The flux corrected transport (FCT) algorithm of Boris and Book [*J. Comput. Phys.* **11** (1973), 38–69] is used to solve the continuity equations for electrons and ions on a non-uniform mesh, to facilitate the study of plasma structure near electrodes. It is shown that extreme (even abrupt) mesh size changes can be accommodated with negligible distortion of a density pulse advecting with a constant velocity. The advection of a pulse by a spatially non-uniform velocity field across a non-uniform mesh also gives results comparable with those for a uniform mesh. A treatment of diffusion on a variable mesh is also developed and is shown to agree well with the analytic solution.

1. INTRODUCTION

Equations describing the drift and diffusion of charged particles in an electric field form the starting point for most theoretical studies of gaseous discharges. In many problems the electric field is controlled by space-charge effects, and must therefore be obtained from a solution of Poisson's equation. In these cases the electric field often varies strongly in both space and time, and precise numerical algorithms are needed to account accurately for charge cancellation in the evaluation of the net charge density. A comparison [1] of several methods that might be used to solve these equations identified several advantages of the flux-corrected transport (FCT) algorithm of Boris and Book [2]. Examples of the application of this algorithm to studies of gaseous discharges may be found in [3, 4].

Near the electrodes the variation of electric field is particularly steep, and the accurate treatment of electrode phenomena usually demands a very fine spatial mesh. Since the body of the discharge plasma rarely exhibits the steep gradients associated with electrodes, an efficient computational algorithm should allow for a non-uniform spatial mesh. In this paper we show how the FCT algorithm may be applied on such a non-uniform mesh, and display a number of test cases which demonstrate the stability and accuracy of the method. The algorithm follows closely the prescription of Boris and Book [5, Eqs. (41)–(48)] and Morrow and Cram [6], with a simple extension to account for diffusion. Since the goal of the present paper is to exhibit the use of FCT on a nonuniform grid, we consider the drift and diffusion of a single species, and do not discuss the application to electrical discharges.

0021-9991/85 $3.00

2. FCT on a Non-uniform Mesh

The prototype equation to be solved is

$$\frac{\partial \rho}{\partial t} = -\frac{\partial}{\partial x}(\rho w) + \frac{\partial}{\partial x}\left(D\frac{\partial \rho}{\partial x}\right), \tag{1}$$

where D is the diffusion coefficient, ρ is the particle density and w the drift velocity. Boris and Book [5] have presented an FCT algorithm which involves both a non-uniform mesh and zone sliding; for our problems, a fixed, non-uniform mesh suffices. Let this mesh be defined as the set $(x_i | i = 1, N)$, so that two interleaved mesh spacings may be specified

$$\delta x_{i+1/2} = x_{i+1} - x_i \tag{2}$$

and

$$\delta x_i = \tfrac{1}{2}(\delta x_{i+1/2} + \delta x_{i-1/2}). \tag{3}$$

In Ref. [6], geometrical arguments involving linear approximations to $\rho(x)$ are used to formulate an FCT algorithm on a non-uniform mesh. An equally heuristic formulation may be obtained by following Boris and Book [5], who began with a general 3-point explicit approximation to the continuity equation

$$\tilde{\rho}_i^{n+1} = a_i \rho_{i-1}^n + b_i \rho_i^n + c_i \rho_{i+1}^n. \tag{4}$$

In this equation, $\tilde{\rho}_i^{n+1}$ is a first approximation to the density at point x_i at time t^{n+1}; this approximation remains to be "corrected" by later steps in the algorithm. Mass will be conserved provided the coefficients satisfy

$$a_{i+1}\rho_i^n + b_i \rho_i^n + c_{i-1}\rho_i^n = \rho_i^n, \tag{5}$$

and $\tilde{\rho}$ can never be negative if a, b and c are all positive.

A particular form of (4) on a non-uniform mesh is

$$\begin{aligned}\tilde{\rho}_i^{n+1} = \rho_i^n &- \frac{1}{2}\left[\frac{\delta x_{i+1/2}}{\delta x_i}\xi_{i+1/2}(\rho_{i+1}^n + \rho_i^n) - \frac{\delta x_{i-1/2}}{\delta x_i}\xi_{i-1/2}(\rho_i^n + \rho_{i-1}^n)\right] \\ &+ \left[\frac{\delta x_{i+1/2}}{\delta x_i} v_{i+1/2}(\rho_{i+1}^n - \rho_i^n) - \frac{\delta x_{i-1/2}}{\delta x_i} v_{i-1/2}(\rho_i^n - \rho_{i-1}^n)\right],\end{aligned} \tag{6}$$

where

$$\begin{aligned} a_i &= \frac{\delta x_{i-1/2}}{\delta x_i}\left(v_{i-1/2} + \frac{1}{2}\xi_{i-1/2}\right), \\ b_i &= \frac{\delta x_{i+1/2}}{\delta x_i}\left(\frac{1}{2} - \frac{1}{2}\xi_{i+1/2} - v_{i+1/2}\right) \\ &\quad + \frac{\delta x_{i-1/2}}{\delta x_i}\left(\frac{1}{2} + \frac{1}{2}\xi_{i-1/2} - v_{i-1/2}\right), \\ c_i &= \frac{\delta x_{i+1/2}}{\delta x_i}(v_{i+1/2} - \tfrac{1}{2}\xi_{i+1/2}). \end{aligned} \tag{7}$$

Equation (6) will satisfy (5) provided

$$\xi_{i+1/2} = w_{i+1/2} \cdot \delta t/\delta x_{i+1/2}, \tag{8}$$

where $w_{i+1/2} = \frac{1}{2}(w_i + w_{i+1})$. Any value of v satisfying

$$v_{i+1/2} \geqslant \frac{1}{2}|\xi_{i+1/2}| \qquad \forall\, i \tag{9}$$

will then ensure that the density is always positive, but algorithms based on this inequality are generally subject to strong numerical diffusion. This defect may be corrected by introducing anti-diffusive fluxes. The simple explicit SHASTA algorithm [5] uses

$$v_{i+1/2} = \frac{1}{8} + \frac{1}{2}\xi^2_{i+1/2}$$

and an anti-diffusive flux

$$\phi_{i+1/2} = \frac{\delta x_{i+1/2}}{\delta x_i}\mu_{i+1/2}(\tilde{\rho}^{n+1}_{i+1} - \tilde{\rho}^{n+1}_i) \tag{10}$$

with $\mu_{i+1/2} = \frac{1}{8}$. A more accurate scheme which is adopted in this paper is the Phoenical LPE SHASTA algorithm [7], which has the following form on a non-uniform mesh:

$$\begin{aligned}
\phi_{i+1/2} = \mu_{i+1/2}\frac{\delta x_{i+1/2}}{\delta x_i}\Bigg[\tilde{\rho}^{n+1}_{i+1} - \tilde{\rho}^{n+1}_i + \frac{1}{6}\Bigg\{ &- \frac{\delta x_{i+3/2}}{\delta x_{i+1}}(\rho^n_{i+2} - \rho^n_{i+1}) \\
&+ \frac{\delta x_{i+1/2}}{\delta x_{i+1}}(\rho^n_{i+1} - \rho^n_i) + \frac{\delta x_{i+1/2}}{\delta x_i}(\rho^n_{i+1} - \rho^n_i) - \frac{\delta x_{i-1/2}}{\delta x_i}(\rho^n_i - \rho^n_{i-1})\Bigg\}\Bigg], \\
\phi_{i-1/2} = \mu_{i-1/2}\frac{\delta x_{i-1/2}}{\delta x_i}\Bigg[\tilde{\rho}^{n+1}_i - \tilde{\rho}^{n+1}_{i-1} + \frac{1}{6}\Bigg\{ &- \frac{\delta x_{i+1/2}}{\delta x_i}(\rho^n_{i+1} - \rho^n_i) \\
&+ \frac{\delta x_{i-1/2}}{\delta x_i}(\rho^n_i - \rho^n_{i-1}) + \frac{\delta x_{i-1/2}}{\delta x_{i-1}}(\rho^n_i - \rho^n_{i-1}) - \frac{\delta x_{i-3/2}}{\delta x_{i-1}}(\rho^n_{i-1} - \rho^n_{i-2})\Bigg\}\Bigg].
\end{aligned} \tag{11}$$

In this algorithm, one chooses

$$v_{i+1/2} = \frac{1}{6} + \frac{1}{3}\varepsilon^2_{i+1/2} \qquad \text{and} \qquad \mu_{i+1/2} = \frac{1}{6}(1 - \varepsilon^2_{i+1/2}). \tag{12}$$

To prevent the antidiffusive scheme from introducing spurious maxima or minima in the solution, or accentuating existing maxima, the antidiffusive flux estimates must be limited. The limiting criteria given by Boris and Book [5, Eq. 20] or Zalesak

[8, Sect. IV] do not need to be modified when applied on a non-uniform grid. We use Zalesak's flux limiting algorithm for our examples below. The limited antidiffusive fluxes $\{\tilde{\phi}_{i+1/2}\}$ may then be used to compute the final value of the updated density

$$\rho_i^{n+1} = \tilde{\rho}_i^{n+1} - \tilde{\phi}_{i+1/2} + \tilde{\phi}_{i-1/2}. \tag{13}$$

3. Diffusion on a Non-uniform Grid

A simple finite difference approximation to the diffusion term in the model equation (1) on a non-uniform mesh is

$$\frac{\partial}{\partial x}\left(D\frac{\rho}{\partial x_i}\right) \approx \frac{(D_{i+1}+D_i)(\rho_{i+1}^n-\rho_i^n)/\delta x_{i+1/2} - (D_i+D_{i-1})(\rho_i^n-\rho_{i-1}^n)/\delta x_{i-1/2}}{\delta x_{i+1/2}+\delta x_{i-1/2}}, \tag{14}$$

where D_i is the (spatially variable) diffusion coefficient at the mesh point x_i. If we define

$$D_{i+1/2} = \frac{1}{2}(D_i + D_{i+1})$$

and (15)

$$\eta_{i+1/2} = \delta t \cdot D_{i+1/2}/\delta x_{i+1/2}^2,$$

the diffusion term by itself gives the following estimate of the updated density:

$$\rho_i^{n+1} = \rho_i^n + \eta_{i+1/2}\frac{\delta x_{i+1/2}}{\delta x_i}(\rho_{i+1}^n - \rho_i^n) - \eta_{i-1/2}\frac{\delta x_{i-1/2}}{\delta x_i}(\rho_i^n - \rho_{i-1}^n). \tag{16}$$

Equation (16) may be used either in Eq. (6), by modifying the coefficients v to

$$v'_{i+1/2} = v_{i+1/2} + \eta_{i+1/2}, \tag{17}$$

or directly after the application of Eq. (13). In the former case, flux-correction is applied to the updated density including the effects of real diffusion. A comparison of the methods on a test problem involving simultaneous transport and diffusion of a Gaussian pulse revealed only small differences, although the alternative described by (17) gave results that were slightly more accurate.

4. Examples

Our first example shows the transport, without diffusion, of a rectangular density pulse across the non-uniform mesh defined by

$$x_i = x_{i-1} + \delta x_i \qquad (i = 2..., N), \tag{18}$$

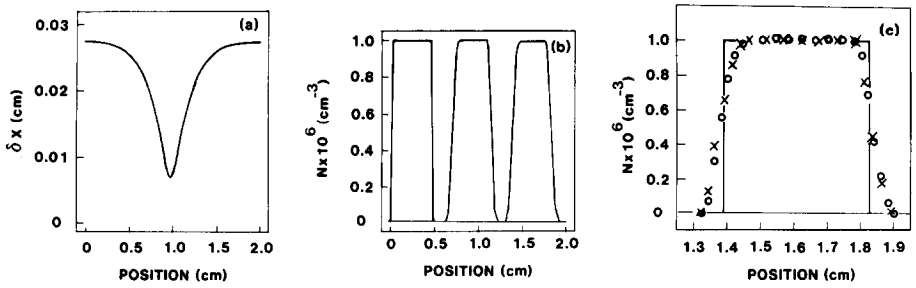

FIG. 1. Results of numerical studies of the transport of a rectangular density pulse over a non-uniform mesh. (a) Mesh variation; (b) square wave propagation from left to right over mesh shown in (a); (c) position of the square wave after 800 time steps or 36.11 nsec: exact solution (—); uniform mesh (O); non-uniform mesh (×).

where $x_1 = 0$, $\delta x_i = 1.0 - 0.75\ \exp(-((i-M)/k)^2)$, $M = (N-1)/2 + 1$, and $K = (N-1)/5$. The mesh is then expanded to give the required value of x_N. In all cases we used $N = 101$ and, except in the variable-velocity case, $w = 3.786 \times 10^8$ cm sec^{-1}.

Figure 1a shows how the mesh spacing varies with x and Fig. 1b shows the form of the pulse as it is transported across the mesh. Figure 1c compares the final pulse shapes from Fig. 1(b) with the corresponding shape at the same time following transport across a uniform N-point mesh. The differences between the pulse after traversing the non-uniform and uniform meshes are due almost entirely to the difficulty of precisely matching the two mesh arrays. It is evident that the pulses traverse the non-uniform grid with no significant distortion, and that no parasitic structures emerge.

Encouraged by this success, we considered a second example involving severe and sudden distortions in the mesh:

$$\begin{aligned} x_i &= x_{i-1} + \delta x \qquad (i = 2, 26) \\ x_i &= x_{i-1} + \delta x/4 \qquad (i = 27, 76), \\ x_i &= x_{i-1} + \delta x \qquad (i = 77, 101), \end{aligned} \tag{19}$$

where δx is adjusted to give the required value of x_N, and $x_1 = 0$.

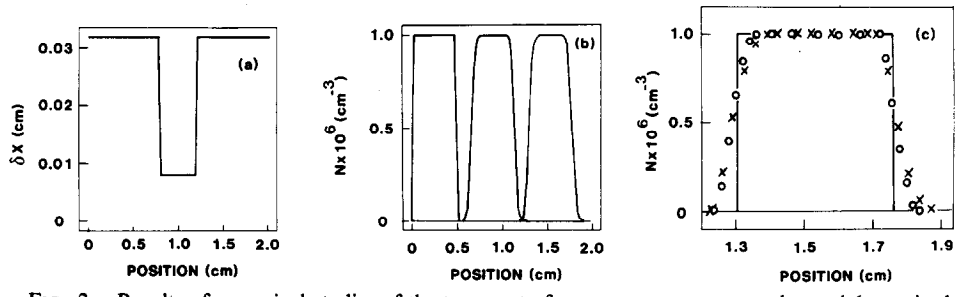

FIG. 2. Results of numerical studies of the transport of a square wave over an abrupt 4:1 step in the mesh size. (a) Step mesh variation; (b) square wave propagation from left to right over mesh shown in (a); (c) comparison of the solutions after 640 time steps or $t = 33.81$ nsec: exact solution (—); uniform mesh (O); step mesh variation (×).

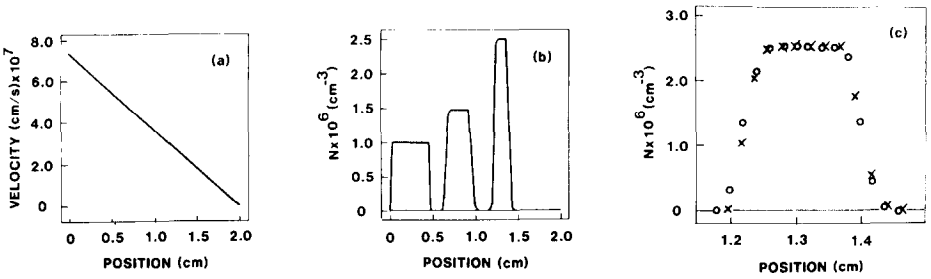

FIG. 3. The transport of a square wave over the mesh shown in Fig. 2a using a spatially dependent velocity field. (a) Velocity variation versus position; (b) square wave propagation from left to right over mesh of Fig. 2a with variation in velocity shown in 4a; (c) comparison of the solution after 540 time steps or $t = 24.61$ nsec: uniform mesh (O); non-uniform mesh (×); both calculated using the same velocity variation.

Figure 2a exhibits the variation of mesh size with x, Fig. 2b shows a rectangular pulse as it traverses the mesh, and Fig. 2c compares the final pulse with the result of transport across a uniform mesh. Although there is evidence of slight perturbations induced by transport across this highly distorted mesh, the algorithm appears to be well-behaved even in this extreme test. We would, however, urge the reader to heed the advice of Zalesak [9], and to use smooth mappings from the index $\{i\}$ to the spatial mesh $\{x_i\}$.

The third example (Fig. 3) shows the transport of a rectangular pulse in the presence of a non-uniform velocity field, across the non-uniform mesh defined by (17). Again, the final pulse compares well with that produced by transport across a uniform mesh.

Our fourth example illustrates a problem similar to those that arise in theoretical

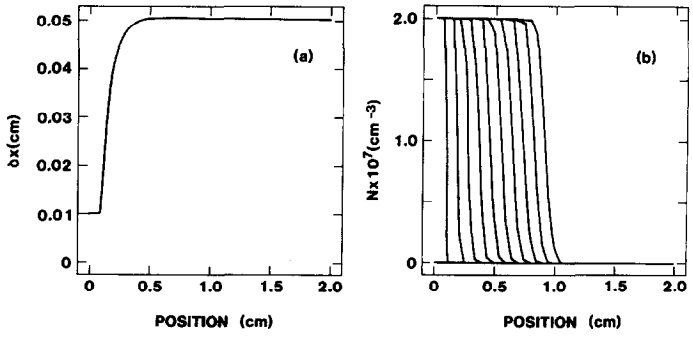

FIG. 4. Application to the problem of a continuous source of electrons at an electrode propagating from left to right into a non-uniform mesh defined by Eq. (35), using fictitious points inside the boundary. (a) Mesh variation; (b) propagation of the electron front from left to right for 24 nsec or 200 time steps.

studies of gas discharges. A non-uniform mesh crowded near the origin (an "electrode") is defined by the transformation

$$\begin{aligned} x_i &= x_{i-1} + 0.2 \qquad (i = 2, 10), \\ x_i &= x_{i-1} + \delta x_i \qquad (i = 11, 101), \end{aligned} \tag{20}$$

where $\delta x_i = 1.0 - 0.8 \exp(-(i-10)^2/25)$, $x_1 = 0$, and the x values are adjusted to give the required value of x_N. Beginning at $t = 0$, a steady flux of particles is emitted from the electrode and transported across the non-uniform mesh into the body of the "plasma." The steady flux at $x_1 = 0$ is modelled by introducing two fictitious mesh points x_{-1} and x_{-2} within the electrode, and then defining the velocity and density at these points by

$$\rho_{-2} = \rho_{-1} = \rho_1$$

and

$$w_{-2} = w_{-1} = w_1 \qquad \text{at time } t. \tag{21}$$

The existence of these fictitious points ensures that the 5-point Phoenical LPE SHASTA algorithm (11) can be implemented without special treatment of points lying near the boundary. Figure 4 shows the mesh spacing and the transport of the step function.

The final example illustrates the diffusion algorithm (16) on the non-uniform mesh (17). The initial pulse has the Gaussian form

$$\rho(x, t = 0) = 10^{10} \exp(-x^2/3.61 \times 10^{-3}), \tag{22}$$

and the diffusion constant used is $D = 5 \times 10^5 \text{ cm}^2 \text{ sec}^{-1}$. Figure 5 compares the analytic solution of the diffusion problem [10] with two numerical solutions, one obtained from a uniform and one from a non-uniform mesh. The algorithm provides an accurate numerical description of diffusion on a non-uniform mesh.

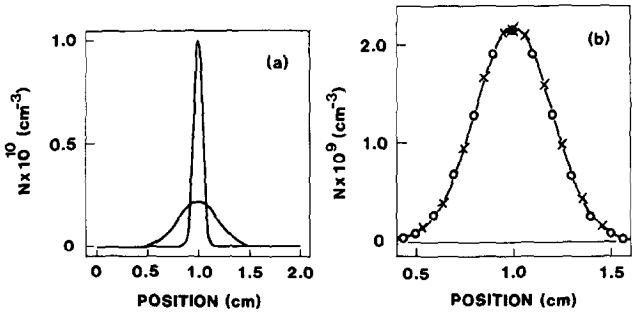

FIG. 5. Comparisons between analytical and numerical solution of the diffusion equation. (a) Initial pulse at $t = 0$ and diffused pulse at $t = 36.11$ nsec, after 800 time steps; (b) comparison of solution after 800 time steps: uniform mesh (O); non-uniform mesh (×); analytic solution (—).

5. Summary

The Phoenical LPE SHASTA algorithm of Boris and Book [5] has been applied to study transport on a non-uniform mesh. Even for an abrupt step change in mesh size of 4:1, there is no sign of the distortions and reflections often referred to in the literature on other treatments of non-uniform meshes. The addition of a variable velocity to the non-uniform mesh does not cause any additional problems. In all cases presented, the total number density of particles is conserved to a very high order of accuracy. The agreement of the analytic solution for diffusion with the numerical solutions on uniform and non-uniform meshes is excellent, showing that diffusion is easily represented on a non-uniform mesh.

Although the FCT algorithm has been found in practice to be sufficiently accurate to meet the rather stringent demands imposed by the presence of space-charge effects in gas discharge problems, it must be noted that the method has not yet been placed on a rigorous analytic foundation. The heuristic character of the algorithm should engender caution in its users, and even greater caution should be exercised in problems on non-uniform meshes, since the truncation errors may be large if the mesh is not chosen appropriately [11]. Our test cases show that the algorithm is very robust, so that great care is needed in confirming the accuracy of results obtained with it.

References

1. R. Morrow, *J. Comput. Phys.* **43** (1981), 1–15.
2. J. P. Boris and D. L. Book, *J. Comput. Phys.* **11** (1973), 38–69.
3. R. Morrow, *J. Comput. Phys.* **46** (1982), 454–461.
4. R. Morrow and J. J. Lowke, "Trichel Pulses in Oxygen: A Simple Theory," 7th International Conference on Gas Discharges, London, 1982.
5. J. P. Boris and D. L. Book, "Methods in Computational Physics" (John Killeen, Ed.), pp. 85–130, Academic Press, New York, 1976.
6. R. Morrow and L. E. Cram, Flux-corrected transport on a non-uniform mesh in plasma boundary problems, *in* "Computational Techniques and Applications" (J. Noye and C. Fletcher, Eds.), pp. 719–729, North–Holland, Amsterdam, 1984.
7. J. P. Boris and D. L. Book, *J. Comput. Phys.* **20** (1976), 397–431.
8. S. T. Zalesak, *J. Comput. Phys.* **31** (1979), 335–362.
9. S. T. Zalesak, "Advances in Computer Methods for Partial Differential Equations-IV" (R. Vichnevetsky and R. S. Stepleman, Eds), IMACS, 1981.
10. F. LLewellyn-Jones, "Ionization and Breakdown in Gases," Wiley, New York, 1957.
11. J. D. Hoffman, *J. Comput. Phys.* **46** (1982), 469–474.